BOUNDARY ELEMENTS MODELLING FOR SMALL/LARGE STRAIN ANALYSIS OF ELASTOMERIC MATERIALS

Dr. Imad A. Hussain
Al-Nahrain University

Prof. Dr. Muhsin J. Jweeg
Al-Nahrain University

Dr. Muhsin N. Hamza
University of Technology

ABSTRACT

In this paper the boundary elements method is used as numerical techniques for solving elastomeric materials (rubber or rubber-like materials) under small and large strains analysis. Under small deformations, the formulations are based on assuming that the elastomer is linear elastic isotropic incompressible solid. While for the large deformation, the formulation is based on decomposing the 1st Piola-Kirchhoff stresses into linear and nonlinear parts. Thereafter, the final derived equations are composed of both boundary integral and non-linear domain integrals. The non-linear analyses were performed using an incremental procedure with an iterative algorithm.

Solving some numerical examples and comparing the results with that obtained from some available results and ANSYS 10.0 showed that the boundary elements method is a good numerical technique for solving incompressible elastomeric materials. And the formulation used for the boundary elements derivations for large strain analysis gave satisfactory results as compared with that of ANSYS ver. 10.0.

الخلاصة

التحقيقات العددية اعتمدت على استخدام طريقة العناصر الحدودية. تم استخدام هذة الطريقة لحل مسائل المواد المطاطية عند التشوهات الصغيرة والتشوهات الكبيرة. اعتمد الاشتقاق الرياضي في التشوهات الصغيرة لهذا النوع من المواد بافتراض ان هذه المواد هي مواد ذات خواص متسقة الاتجاهات، خطية، مرنة، ولاانضغاطية. بينما اعتمد الاشتقاق الرياضي تحت التشوهات الكبيرة على اساس فصل الاجهادات الكلية او اجهادات بايلا–كرشوف الاولى الى جزء خطي وجزء لاخطي. بناءا عليه، فان المعادلات النهائية احتوت على تكاملات محيطية وتكاملات ميدانية. تم الحصول على الحلول في الجزء اللاخطي بالاعتماد على اسلوب عددي يحوي على اجراءات تزايدية للحمل مع خوارزمية تكرارية، اثبتت المقارنات عند حل بعض المسائل العددية ان طريقة العناصر الحدودية اكثر ملائمة من الطرق الاخرى لحل المسائل الخاصة بالمواد اللاانضغاطية. كذلك اثبت ان الاشتاق الخاص بالتشوهات الكبيرة للعناصر الحدودية صحيح واعطى نتائج مرضية عند مقارنته مع طرائق العناصر المحددة مثل الـ ANSYS.

KEYWORD: rubber or rubber-like, elastomers, BEM, incompressible materials, large strain, hyperelastic

INTRODUCTION

Successful analysis of elastomers (rubber or rubber-like materials) requires robust numerical methods and representative material models applicable to small/large strains and multiple deformation modes. Although the mathematical foundation of strain energy density function has been studied by many researchers, the application to engineering problems is not straightforward.

Two major challenges are encountered in the numerical analysis of rubber materials. The first is due to the material incompressibility of rubber. The material incompressibility leads to a locking difficulty when using the conventional finite element method. The finite element prediction is often much stiffer (locking) than analytical solution or experimental data resulting from the imposition of "constant volume constraint" in the numerical formulation. Locking usually accompanies with pressure oscillation that completely corrupts the numerical stress solution, Herrmann 1985. The second difficulty is the mesh distortion caused by the large deformation nature in many elastomeric applications. Therefore it is necessary to search for other numerical techniques that may help in getting improved numerical analysis. In this work the boundary elements method has been chosen as numerical technique for solving elastomeric problems.

The boundary elements method is relatively a new technique and successfully applied to many engineering problems. The most remarkable feature of these methods are that instead of attempting to find an approximate solution for the governing differential equations throughout the relevant solution domain, as in the domain methods, the equations are converted into an integral form, often involving only integrals over the boundary of the domain, consequently, only the boundary has to be discretised in order to carry out the integration. Although these methods successfully applied to many engineering problems have had limited application with elastomers, Polyzos 1998.

The lack of inaccurate results of the conventional finite element method is due to Poisson’s ratio values in elastomers, which ranges between 0.499 and 0.5. The elements used in FEA need to be reformulated to accommodate this high value of Poisson's ratio. This is usually accomplished by utilizing an approach developed by Herrmann 1985, by introducing a new variational principle that includes another degree of freedom called the “mean pressure function.” When using the boundary elements method there is no such restriction and the method can handle elastomeric materials or generally incompressible materials accurately.

When managing elastomeric components using the boundary elements method, or any numerical technique, two major decisions will present themselves:

- Is a nonlinear analysis required, or will a linear analysis suffice?
- What material properties will be used?

These two decisions are interrelated, and the answer depends on what application the elastomeric components are designed for.

Keeping this in mind, therefore, one has to adopt either linear or non-linear analyses. As a result, in the present work, the boundary elements method is applied to elastomers by considering both small and large deformations. For small deformation the formulation is considered by assuming that the elastomers are linear elastic isotropic axisymmetric solids. The derivations lead to

a fact that only the boundary of the region being investigated has to be discretised. In large, or finite, deformation elastomers are considered to be hyperelastic solids, and nonlinear boundary elements method has been used. The derivations of the boundary integral equations were done by splitting the first Piola-Kirchoff stresses or total stresses into linear and non-linear components. Thereafter, the final derived equations are composed of both boundary integral and non-linear domain integration terms, consequently, both the boundary and the domain of the problem are discretised.

SMALL DEFORMATION BEM

In this section rubber components are considered under small deformations or small strains. A good approximation for the corresponding stresses is given by conventional elastic analysis, assuming simple linear stress-strain relationships, because, like all solids, rudder behaves as a linearly elastic substance at relatively small strains, Gent 2001. When applying the boundary elements technique to an axisymmetric elastomeric solid under axisymmetric loading and by taking the advantage of symmetry, the original three-dimensional problem will be reduced to a two-dimensional one. Therefore, it is only required to discretise the boundary of the radial plane, as shown in Fig. 1.

The boundary integral equation, BIE, can be obtained using weighted residual technique. Now, consider that one desire to minimize the error involved in the numerical approximation of the governing equations of axisymmetric solid;

$$\frac{\partial \sigma_r}{\partial r} + \frac{\partial \tau_{rz}}{\partial z} + \frac{\sigma_r - \sigma_\theta}{r} + \beta_r = 0$$

$$\frac{\partial \tau_{rz}}{\partial r} + \frac{\partial \sigma_z}{\partial z} + \frac{\tau_{rz}}{r} + \beta_z = 0$$

Which usually have to satisfy the essential and the natural boundary conditions.

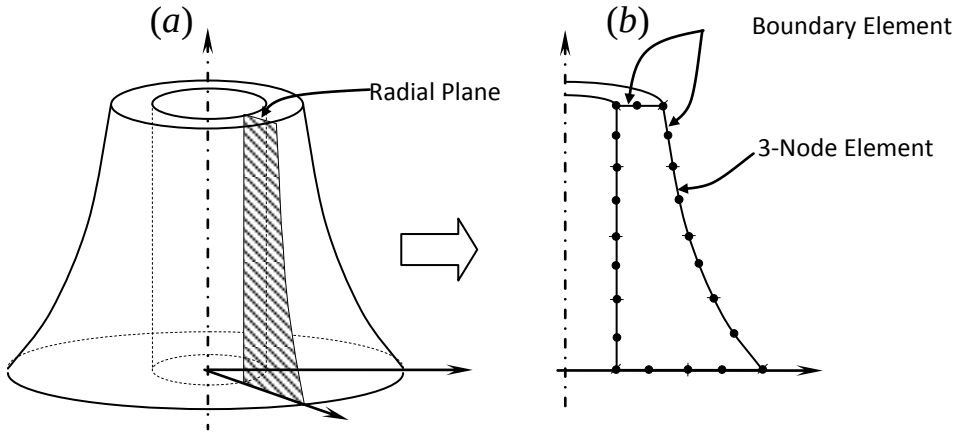

Figure 1: Discretisation of axisymmetric solid using BEM;
(*a*) original 3D problem, (*b*) radial plane BEM mesh

Minimizing the above equations by displacement type functions u^* and v^* using weighted residual technique as;

$$\iint_{\Omega}\left(\frac{\partial\sigma_r}{\partial r}+\frac{\partial\tau_{rz}}{\partial z}+\frac{\sigma_r-\sigma_\theta}{r}+\beta_r\right)u^*\,\mathrm{d}\Omega+\iint_{\Omega}\left(\frac{\partial\tau_{rz}}{\partial r}+\frac{\partial\sigma_z}{\partial z}+\frac{\tau_{rz}}{r}+\beta_z\right)v^*\,\mathrm{d}\Omega=0 \tag{1}$$

where $d\Omega = 2\pi\, r\, dr\, dz$, carrying out the integration by parts for each term separately leads to

$$\begin{aligned}&\int_{\Gamma}\sigma_r\,u^*n_r\,r\,d\Gamma-\iint_{\Omega}\sigma_r\frac{\partial}{\partial r}(u^*r)\,dr\,dz+\int_{\Gamma}\tau_{rz}\,u^*n_z\,r\,d\Gamma-\int_{\Gamma}\sigma_r\,u^*n_r\,r\,d\Gamma-\iint_{\Omega}\sigma_r\frac{\partial}{\partial r}(u^*r)\,dr\,dz\\&+\int_{\Gamma}\tau_{rz}\,u^*n_z\,r\,d\Gamma-\iint_{\Omega}\tau_{rz}\frac{\partial u^*}{\partial z}r\,dr\,dz+\iint_{\Omega}\frac{\sigma_r-\sigma_\theta}{r}u^*r\,dr\,dz+\int_{\Gamma}\tau_{rz}\,v^*n_r\,r\,d\Gamma-\iint_{\Omega}\tau_{rz}\frac{\partial}{\partial r}(r\,v^*)dr\,dz\\&+\int_{\Gamma}\sigma_z\,v^*n_z\,r\,d\Gamma-\iint_{\Omega}\sigma_z\frac{\partial v^*}{\partial r}r\,dr\,dz+\iint_{\Omega}\frac{\tau_{rz}}{r}v^*r\,dr\,dz+\iint_{\Omega}(\beta_r u^*+\beta_z v^*)r\,dr\,dz=0\end{aligned} \tag{2}$$

Further simplifications and rearranging, gives

$$\begin{aligned}&\int_{\Gamma}(\sigma_r\,n_r+\tau_{rz}\,n_z)u^*\,r\,d\Gamma+\int_{\Gamma}(\tau_{rz}\,n_r+\sigma_z\,n_z)v^*\,r\,d\Gamma-\iint_{\Omega}(\sigma_r\frac{\partial u^*}{\partial r}+\sigma_z\frac{\partial v^*}{\partial z})r\,dr\,dz\\&-\iint_{\Omega}\tau_{rz}(\frac{\partial u^*}{\partial z}+\frac{\partial v^*}{\partial r})r\,dr\,dz-\iint_{\Omega}\sigma_r(\frac{u^*}{r}+\frac{v^*}{r})r\,dr\,dz+\iint_{\Omega}\frac{\sigma_r-\sigma_\theta}{r}u^*r\,dr\,dz\\&+\iint_{\Omega}\frac{\tau_{rz}}{r}v^*r\,dr\,dz+\iint_{\Omega}(\beta_r u^*+\beta_z v^*)r\,dr\,dz=0\end{aligned} \tag{3}$$

Define

$$\boldsymbol{\varepsilon}^*=\{\varepsilon_r^*,\varepsilon_z^*,\varepsilon_\theta^*,\gamma_{rz}^*\}\quad\text{and}\quad\boldsymbol{\sigma}=\{\sigma_r,\sigma_z,\sigma_\theta,\tau_{rz}\} \tag{4}$$

This leads to

$$\int_{\Gamma}(t_r\,u^*+t_z\,v^*)\,r\,d\Gamma-\iint_{\Omega}(\sigma_r\varepsilon_r^*+\sigma_z\varepsilon_z^*+\sigma_\theta\varepsilon_\theta^*+\tau_{rz}\gamma_{rz}^*)r\,dr\,dz+\iint_{\Omega}(\beta_r u^*+\beta_z v^*)r\,dr\,dz=0$$

or in a vectorial form

$$\int_{\Gamma}(t_r\,u^*+t_z\,v^*)\,r\,d\Gamma-\iint_{\Omega}\boldsymbol{\varepsilon}^{*T}\boldsymbol{\sigma}\,r\,dr\,dz+\iint_{\Omega}(\beta_r u^*+\beta_z v^*)r\,dr\,dz=0 \tag{5}$$

For linear elastic solids, $\boldsymbol{\varepsilon}^{*T}\boldsymbol{\sigma}=\boldsymbol{\varepsilon}^{*T}\mathbf{D}\,\boldsymbol{\varepsilon}$, and since **D** is a symmetric matrix, therefore **D**=$\mathbf{D}^{\mathrm{T}}$, subsequently

$$\boldsymbol{\varepsilon}^{*T}\boldsymbol{\sigma}=\boldsymbol{\varepsilon}^{*T}\mathbf{D}^{T}\,\boldsymbol{\varepsilon}=\boldsymbol{\sigma}^{*T}\boldsymbol{\varepsilon}$$

Substitute above into equation (5), leads to

$$\int_{\Gamma}(t_r\,u^*+t_z\,v^*)\,r\,d\Gamma-\iint_{\Omega}(\sigma_r^*\varepsilon_r+\sigma_z^*\varepsilon_z+\sigma_\theta^*\varepsilon_\theta+\tau_r^*\gamma_{rz})r\,dr\,dz+\iint_{\Omega}(\beta_r u^*+\beta_z v^*)r\,dr\,dz=0 \tag{6}$$

The first domain integral of the above equation can further be simplified by integrating by parts getting the following equation:

$$\int_{\Gamma}(t_r\,u^* + t_z\,v^*)\,r\,\mathrm{d}\Gamma - \int_{\Gamma}(t_r^*\,u + t_z^*\,v)\,r\,\mathrm{d}\Gamma + \iint_{\Omega}\left(\frac{\partial\sigma_r^*}{\partial r} + \frac{\partial\tau_{rz}^*}{\partial z} + \frac{\sigma_r^* - \sigma_\theta^*}{r}\right)u\,r\,\mathrm{d}r\,\mathrm{d}z + \iint_{\Omega}\left(\frac{\partial\tau_{rz}^*}{\partial r} + \frac{\partial\sigma_z^*}{\partial z} + \frac{\tau_{rz}^*}{r}\right)v\,r\,\mathrm{d}r\,\mathrm{d}z + \iint_{\Omega}(\beta_r u^* + \beta_z v^*)r\,dr\,dz = 0 \tag{7}$$

Eq. (7) represents the inverse wieghted residual expression, which can be used to obtain the boundary integral equation. Considering now a ring source load $\beta_j = \Delta^i \mathbf{e}_j$ applied at a point $i(r_i, z_i)$ in an infinte domain, in the direction of the unit vector $\mathbf{e}_j$, where j=r , z, i.e.

$$\begin{aligned}\frac{\partial\sigma_r^*}{\partial r} + \frac{\partial\tau_{rz}^*}{\partial z} + \frac{\sigma_r^* - \sigma_\theta^*}{r} + \Delta^i\mathbf{e}_r = 0\\ \frac{\partial\tau_{rz}^*}{\partial r} + \frac{\partial\sigma_z^*}{\partial z} + \frac{\tau_{rz}^*}{r} + \Delta^i\mathbf{e}_z = 0\end{aligned} \tag{8}$$

where i refer to the point at which the load is applied, Δ^i is the Dirac delta function, which is define as, Kyuichiro Washizo 1975;

$$\Delta^i = \begin{cases}[\text{singular at point i}]\\ 0\,[\text{at any other point}]\end{cases} \tag{9}$$

and Δ^i has the following property:

$$\iint_{\Omega}\Delta^i(p,Q)\,\mathbf{u}_{\mathrm{i}}(Q)\,d\Omega = C_i u(p) \tag{10}$$

where

$$C_i = \begin{cases}1 & if \quad p \in \Omega\\ 0 & if \quad p \notin \Omega + \Gamma\\ 0.5 & if \quad p \text{ is on smooth continuous boundary } \Gamma\\ \dfrac{\alpha_i}{2\pi} & if \quad p \text{ is on a corner of angle } \alpha_i \text{ on the boundary } \Gamma\end{cases}$$

Substiute eq. (8) into eq. (7) one get

$$\int_{\Gamma}(t_r\,u^* + t_z\,v^*)\,r\,d\Gamma - \int_{\Gamma}(t_r^*\,u + t_z^*\,v)\,r\,d\Gamma - \iint_{\Omega}\Delta^i\mathbf{e}_r\,u\,d\Omega - \iint_{\Omega}\Delta^i\mathbf{e}_z v\,d\Omega + \iint_{\Omega}(\beta_r u^* + \beta_z v^*)r\,dr\,dz = 0 \tag{11}$$

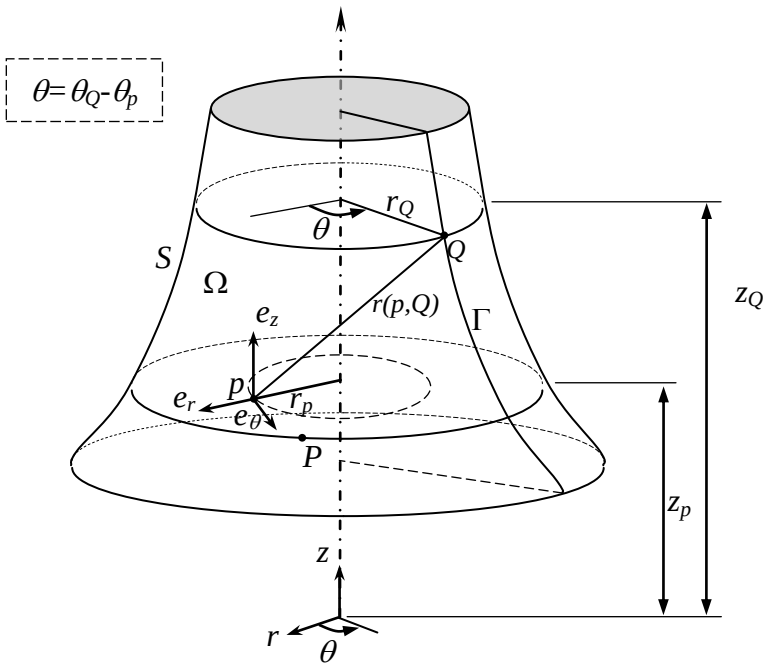

Figure 2: Domain of axisymmetric solid.

Consider each direction independently, the displacement at any point in the infinite domain is;

$$\begin{aligned} u^* &= U_{rr}\mathbf{e}_r + U_{zr}\mathbf{e}_z \\ v^* &= U_{rz}\mathbf{e}_r + U_{zz}\mathbf{e}_z \end{aligned} \tag{12}$$

$\mathbf{e}_r, \mathbf{e}_z$ is the components of the ring loads at point p in r and z direction, respectively, as shown in Fig. 2. U_{rr}, U_{rz}, U_{zr} and U_{zz} are displacement kernel functions. The first subscript refers to the direction of the displacement at the boundary point Q (feild point), while the second refers to the direction of the ring load at point p (source point) causing the displacement at Q.

Similarly, the traction vector components at Q can be expressed as:

$$\begin{aligned} t_r^* &= T_{rr}\mathbf{e}_r + T_{zr}\mathbf{e}_z \\ t_z^* &= T_{rz}\mathbf{e}_r + T_{zz}\mathbf{e}_z \end{aligned} \tag{13}$$

where T_{rr}, T_{rz}, T_{zr} and T_{zz} are the traction kernels.

Substitute eq. (12) and eq. (13) into eq. (11), gives

$$\begin{aligned} &\int_\Gamma \left[t_r\,(U_{rr}\mathbf{e}_r + U_{zr}\mathbf{e}_z) + t_z\,(U_{rz}\mathbf{e}_r + U_{zz}\mathbf{e}_z)\right] r\,d\Gamma - \int_\Gamma \left[(T_{rr}\mathbf{e}_r + T_{zr}\mathbf{e}_z)\,u + (T_{rz}\mathbf{e}_r + T_{zz}\mathbf{e}_z)v\right] r\,d\Gamma \\ &- \iint_\Omega \Delta^i \mathbf{e}_r\,u\,d\Omega - \iint_\Omega \Delta^i \mathbf{e}_z v\,d\Omega + \iint_\Omega \left[\beta_r (U_{rr}\mathbf{e}_r + U_{zr}\mathbf{e}_z) + \beta_z (U_{rz}\mathbf{e}_r + U_{zz}\mathbf{e}_z)\right] r\,dr\,dz = 0 \end{aligned} \tag{14}$$

Since $\mathbf{e}_r$ and $\mathbf{e}_z$ are independent on each other, then eq. (14) can be split as:

$$\int_{\Gamma}\left(t_r\,U_{rr}+t_z\,U_{rz}\right)r\,d\Gamma-\int_{\Gamma}\left(T_{rr}\,u+T_{rz}\,v\right)r\,d\Gamma-\iint_{\Omega}\Delta^i\,u\,d\Omega+\iint_{\Omega}\left(\beta_r\,U_{rr}+\beta_z\,U_{rz}\right)d\Omega=0 \tag{15}$$

and

$$\int_{\Gamma}\left(t_r\,U_{zr}+t_z\,U_{zz}\right)r\,d\Gamma-\int_{\Gamma}\left(T_{zr}\,u+T_{zz}v\right)r\,d\Gamma-\iint_{\Omega}\Delta^i\,v\,d\Omega+\iint_{\Omega}\left(\beta_r\,U_{zr}+\beta_z\,U_{zz}\right)d\Omega=0 \tag{16}$$

When the source point is at an interior point '*p'* then equations (15) and (16) lead to Somiglianna's identity, Rizzo and Shippy 1986, defined as:

$$\begin{aligned}u(p)=&\int_{\Gamma}\left(t_r(Q)\,U_{rr}(p,Q)+t_z(Q)\,U_{rz}(p,Q)\right)r_Q\,d\Gamma-\\&\int_{\Gamma}\left(T_{rr}(p,Q)\,u(Q)+T_{rz}(p,Q)\,v(Q)\right)r_Q\,d\Gamma+\iint_{\Omega}\left(\beta_r\,U_{rr}(p,Q)+\beta_z\,U_{rz}(p,Q)\right)d\Omega\end{aligned} \tag{17}$$

and

$$\begin{aligned}v(p)=&\int_{\Gamma}\left(t_r(Q)\,U_{zr}(p,Q)+t_z(Q)\,U_{zz}(p,Q)\right)r_Q\,\mathrm{d}\Gamma-\\&\int_{\Gamma}\left(T_{zr}(p,Q)\,u(Q)+T_{zz}(p,Q)\,v(Q)\right)r_Q\,\mathrm{d}\Gamma+\iint_{\Omega}\left(\beta_r\,U_{zr}(p,Q)+\beta_z\,U_{zz}(p,Q)\right)\mathrm{d}\Omega\end{aligned} \tag{18}$$

The above equations give the displacement components at an interior point *p*. To find the final boundary integral equation, each term in equations (17) and (18) is taken to the limits as the interior point *p* approach the boundary point *P*, i.e. $p\rightarrow P$. Therefore, these integral equations have now a singularity and the integral on Γ is defined only in the sense of the Cauchy principal value, Rizzo and Shippy 1986, and Brebbia 1989, resulting the following:

$$C_{rr}u^i+C_{rz}v^i+\int_{\Gamma}\left(T_{rr}\,u+T_{rz}\,v\right)r_Q\,d\Gamma=\int_{\Gamma}\left(t_r\,U_{rr}+t_z\,U_{rz}\right)r_Q\,d\Gamma+\iint_{\Omega}\left(\beta_r\,U_{rr}+\beta_z\,U_{rz}\right)d\Omega=0 \tag{19}$$

and

$$C_{zr}u^i+C_{zz}v^i+\int_{\Gamma}\left(T_{zr}\,u+T_{zz}\,v\right)r_Q\,d\Gamma=\int_{\Gamma}\left(t_r\,U_{zr}+t_z\,U_{zz}\right)r_Q\,d\Gamma+\iint_{\Omega}\left(\beta_r\,U_{zr}+\beta_z\,U_{zz}\right)d\Omega=0 \tag{20}$$

or in a matrix form

$$\begin{bmatrix}C_{rr}&C_{rz}\\C_{zr}&C_{zz}\end{bmatrix}\begin{bmatrix}u^i\\v^i\end{bmatrix}+\int_{\Gamma}\begin{bmatrix}T_{rr}&T_{rz}\\T_{zr}&T_{zz}\end{bmatrix}\begin{bmatrix}u\\v\end{bmatrix}r_Q\,\mathrm{d}\Gamma=\int_{\Gamma}\begin{bmatrix}U_{rr}&U_{rz}\\U_{zr}&U_{zz}\end{bmatrix}\begin{bmatrix}t_r\\t_z\end{bmatrix}r_Q\,\mathrm{d}\Gamma+\iint_{\Omega}\begin{bmatrix}U_{rr}&U_{rz}\\U_{zr}&U_{zz}\end{bmatrix}\begin{bmatrix}\beta_r\\\beta_z\end{bmatrix}r_Q\,\mathrm{d}\Gamma \tag{21}$$

where C_{rr}, C_{rz}, C_{zr} and C_{zz} can be determined from the nature of the boundary geometry at "*P"*, and the value of C_{ij} (*i,j=r, z*) equal unity at interior point and $C_{ij}=\delta_{ij}/2$, (δ_{ij} is the Krönecker delta), when the boundary at *P* is smooth, i.e. have unique tangent at *P*, but can be expressed generally using rigid body motion, Nouri and Husain 2000.

LARGE DEFORMATION BEM

The large deformation BEM derivation, also, will starts from minimizing the error involved in the numerical approximation of the governing differential equations of axisymmetric solid;

$$\begin{aligned}&\frac{\partial \sigma_r}{\partial r}+\frac{\partial \tau_{rz}}{\partial z}+\frac{\sigma_r-\sigma_\theta}{r}+\beta_r=0\\&\frac{\partial \tau_{rz}}{\partial r}+\frac{\partial \sigma_z}{\partial z}+\frac{\tau_{rz}}{r}+\beta_z=0\end{aligned} \tag{22}$$

where β_r and β_z are the radial and axial body forces, the stresses in eq. (22) is the first Piola-Kirchoff stresses or total stresses and can be split into linear and non-linear components as follows:

$$\sigma_{ij}=\sigma_{ij}^{nl}+\sigma_{ij}^{l} \tag{23}$$

where the superscript *nl* refers to non-linear component and the superscript *l* refer to the linear one.

Therefore, equations (22) can now be rewritten as follows:

$$\begin{aligned}&\frac{\partial \sigma_r^l}{\partial r}+\frac{\partial \tau_{rz}^l}{\partial z}+\frac{\sigma_r^l-\sigma_\theta^l}{r}+f_r^{nl}+\beta_r=0\\&\frac{\partial \tau_{rz}^l}{\partial r}+\frac{\partial \sigma_z^l}{\partial z}+\frac{\tau_{rz}^l}{r}+f_z^{nl}+\beta_z=0\end{aligned} \tag{24}$$

where;

$$f_r^{nl}=\frac{\partial \sigma_r^{nl}}{\partial r}+\frac{\partial \tau_{rz}^{nl}}{\partial z}+\frac{\sigma_r^{nl}-\sigma_\theta^{nl}}{r},\quad \text{and}\quad f_z^{nl}=\frac{\partial \tau_{rz}^{nl}}{\partial r}+\frac{\partial \sigma_z^{nl}}{\partial z}+\frac{\tau_{rz}^{nl}}{r}$$

Minimizing equations. (24) by displacement type functions u^* and v^* as:

$$\iint_\Omega\left(\frac{\partial \sigma_r^l}{\partial r}+\frac{\partial \tau_{rz}^l}{\partial z}+\frac{\sigma_r^l-\sigma_\theta^l}{r}+f_r^{nl}+\beta_r\right)u^*\mathrm{d}\Omega+\iint_\Omega\left(\frac{\partial \tau_{rz}^l}{\partial r}+\frac{\partial \sigma_z^l}{\partial z}+\frac{\tau_{rz}^l}{r}+f_z^{nl}+\beta_z\right)v^*\mathrm{d}\Omega=0 \tag{25}$$

Using integration by parts and rearranging gives:

$$\begin{aligned}&\int_\Gamma\left(\sigma_r^l\,n_r+\tau_{rz}^l\,n_z\right)u^*\,r\,d\Gamma+\int_\Gamma\left(\tau_{rz}^l\,n_r+\sigma_z^l\,n_z\right)v^*\,r\,d\Gamma\\&-\iint_\Omega\left(\sigma_r^l\frac{\partial u^*}{\partial r}+\sigma_z^l\frac{\partial v^*}{\partial z}+\sigma_\theta^l\frac{u^*}{r}+\tau_{rz}^l\left(\frac{\partial v^*}{\partial r}+\frac{\partial u^*}{\partial z}\right)\right)r\,dr\,dz\\&+\iint_\Omega\left(f_r^{nl}\,u^*+f_z^{nl}\,v^*\right)r\,dr\,dz+\iint_\Omega\left(\beta_r\,u^*+\beta_z\,v^*\right)r\,dr\,dz=0\end{aligned} \tag{26}$$

writing

$$\begin{aligned}&t_r^l=\sigma_r^l n_r+\tau_{rz}^l n_z,\qquad t_z^l=\tau_{rz}^l n_r+\sigma_z^l n_z,\\&\boldsymbol{\varepsilon}^*=\left\{\varepsilon_r^*,\varepsilon_z^*,\varepsilon_\theta^*,\gamma_{rz}^*\right\},\ \text{and}\ \boldsymbol{\sigma}=\left\{\sigma_r^l,\sigma_z^l,\sigma_\theta^l,\tau_{rz}^l\right\},\end{aligned}$$

where:

$$\varepsilon_r^* = \frac{\partial u^*}{\partial r}; \qquad \varepsilon_\theta^* = \frac{u^*}{r}; \qquad \varepsilon_z^* = \frac{\partial v^*}{\partial z}; \qquad \gamma_{rz}^* = \frac{\partial u^*}{\partial z} + \frac{\partial v^*}{\partial r}$$

Substitute the above expressions, into equation (26) gives;

$$\begin{aligned} &\int_\Gamma \left(t_r^l\, u^* + t_z^l\, v^*\right) r\, d\Gamma - \iint_\Omega \left(\sigma_r \varepsilon_r^* + \sigma_z \varepsilon_z^* + \sigma_\theta \varepsilon_\theta^* + \tau_{rz}\gamma_{rz}^*\right) r\, dr\, dz \\ &+ \iint_\Omega \left(f_r^{nl} u^* + f_z^{nl} v^*\right) r\, dr\, dz + \iint_\Omega \left(\beta_r u^* + \beta_z v^*\right) r\, dr\, dz = 0 \end{aligned} \tag{27}$$

Neglecting the body forces, i.e. $\beta_r = \beta_z = 0$, eq. (27) can be writtin in vectorial form as:

$$\int_\Gamma \left(t_r^l\, u^* + t_z^l\, v^*\right) r\, d\Gamma - \iint_\Omega \left(\boldsymbol{\varepsilon}^{*T} \boldsymbol{\sigma}^l\right) r\, dr\, dz + \iint_\Omega \left(f_r^{nl} u^* + f_z^{nl} v^*\right) r\, dr\, dz = 0 \tag{28}$$

For the linear $\boldsymbol{\sigma}^l$:

$$\boldsymbol{\varepsilon}^{*T} \boldsymbol{\sigma} = \boldsymbol{\varepsilon}^{*T} \mathbf{D}^l\, \boldsymbol{\varepsilon} = \boldsymbol{\sigma}^{*T} \boldsymbol{\varepsilon}^l$$

where $\boldsymbol{\sigma}^* = \left\{\sigma_r^*, \sigma_z^*, \sigma_\theta^*, \tau_{rz}^*\right\} = \mathbf{D}^l\, \boldsymbol{\varepsilon}^*$

Therefore, eq. (28) can be written as:

$$\int_\Gamma \left(t_r^l\, u^* + t_z^l\, v^*\right) r\, d\Gamma - \iint_\Omega \left(\sigma_r^* \varepsilon_r + \sigma_z^* \varepsilon_z + \sigma_\theta^* \varepsilon_\theta + \tau_{rz}^* \gamma_{rz}\right) r\, dr\, dz + \iint_\Omega \left(f_r^{nl} u^* + f_z^{nl} v^*\right) r\, dr\, dz = 0 \tag{29}$$

The first domain integral of the above equation can further simplified by integrating by parts, and equation (29) will be as follows:

$$\begin{aligned} &\int_\Gamma \left(t_r^l\, u^* + t_z^l\, v^*\right) r\, d\Gamma - \int_\Gamma \left(t_r^*\, u + t_z^*\, v\right) r\, d\Gamma + \iint_\Omega \left(\frac{\partial \sigma_r^*}{\partial r} + \frac{\partial \tau_{rz}^*}{\partial z} + \frac{\sigma_r^* - \sigma_\theta^*}{r}\right) u\, r\, dr\, dz + \iint_\Omega \left(\frac{\partial \tau_{rz}^*}{\partial r} + \frac{\partial \sigma_z^*}{\partial z} + \frac{\tau_{rz}^*}{r}\right) v\, r\, dr\, dz \\ &+ \iint_\Omega \left(f_r^{nl} u^* + f_z^{nl} v^*\right) r\, dr\, dz = 0 \end{aligned} \tag{30}$$

Eq. (30) represents the inverse wieghted residual expression. Considering a ring source load $\beta_m = \Delta^i \mathbf{e}_m$ applied at a point $i(r_i, z_i)$ in an infinte domain, in the direction of the unit vector $\mathbf{e}_m$, where *m*=*r*, *z*, i.e.

$$\begin{aligned} \frac{\partial \sigma_r^*}{\partial r} + \frac{\partial \tau_{rz}^*}{\partial z} + \frac{\sigma_r^* - \sigma_\theta^*}{r} + \Delta^i \mathbf{e}_r = 0 \\ \frac{\partial \tau_{rz}^*}{\partial r} + \frac{\partial \sigma_z^*}{\partial z} + \frac{\tau_{rz}^*}{r} + \Delta^i \mathbf{e}_z = 0 \end{aligned} \tag{31}$$

where *i* refers to the point at which the load is applied, Δ^i is the Dirac delta function.

Therefore eq. (30) will be

$$\int_{\Gamma}\left(t_r^l\, u^* + t_z^l\, v^*\right) r\, d\Gamma - \int_{\Gamma}\left(t_r^*\, u + t_z^*\, v\right) r\, d\Gamma - \iint_{\Omega} \Delta^i\, \mathbf{e}_r\, u\, r\, dr\, dz - \iint_{\Omega} \Delta^i\, \mathbf{e}_z\, v\, r\, dr\, dz + \iint_{\Omega} (f_r^{nl} u^* + f_z^{nl} v^*) r\, dr\, dz = 0 \tag{32}$$

From the property of Dirac delta function, eq. (10), eq. (32) gives the nonlinear boundary integral equations of axisymmetric elastomeric solids sustaining large or hyperelastic deformation:

$$C_i u_i \mathbf{e}_r + C_i u_i \mathbf{e}_r + \int_{\Gamma}\left(t_r^*\, u + t_z^*\, v\right) r\, d\Gamma = \int_{\Gamma}\left(t_r^l\, u^* + t_z^l\, v^*\right) r\, d\Gamma + \iint_{\Omega} (f_r^{nl} u^* + f_z^{nl} v^*) r\, dr\, dz \tag{33}$$

The domain integral of equation (33) represnts the non-linear part of this equation. This domain integral is defined as:

$$\iint_{\Omega} (f_r^{nl} u^* + f_z^{nl} v^*) r\, dr\, dz = \iint_{\Omega}\left(\frac{\partial \sigma_r^{nl}}{\partial r} + \frac{\partial \tau_{rz}^{nl}}{\partial z} + \frac{\sigma_r^{nl} - \sigma_\theta^l}{r}\right) u^* r\, dr\, dz + \iint_{\Omega}\left(\frac{\partial \tau_{rz}^{nl}}{\partial r} + \frac{\partial \sigma_z^{nl}}{\partial z} + \frac{\tau_{rz}^{nl}}{r}\right) v^* r\, dr\, dz$$

Integrating by parts and rearranging

$$\iint_{\Omega} (f_r^{nl} u^* + f_z^{nl} v^*) r\, dr\, dz = \int_{\Gamma} (\sigma_r^{nl}\, n_r + \tau_{rz}^{nl}\, n_z) u^*\, r\, d\Gamma + \int_{\Gamma} (\tau_{rz}^{nl}\, n_r + \sigma_z^{nl}\, n_z) v^*\, r\, d\Gamma - \iint_{\Omega}\left(\sigma_r^{nl}\frac{\partial u^*}{\partial r} + \sigma_z^{nl}\frac{\partial v^*}{\partial z} + \sigma_\theta^{nl}\frac{u^*}{r} + \tau_{rz}^{nl}\left(\frac{\partial u^*}{\partial z} + \frac{\partial v^*}{\partial r}\right)\right) r\, dr\, dz$$

since $t_r = \sigma_r n_r + \tau_{rz} n_z$, and $t_z = \tau_{rz} n_r + \sigma_z n_z$, therefore

$$\iint_{\Omega} (f_r^{nl} u^* + f_z^{nl} v^*) r\, dr\, dz = \int_{\Gamma} (t_r^{nl}\, u^* + t_z^{nl}\, v^*)\, r\, d\Gamma - \iint_{\Omega}\left(\sigma_r^{nl}\frac{\partial u^*}{\partial r} + \sigma_z^{nl}\frac{\partial v^*}{\partial z} + \sigma_\theta^{nl}\frac{u^*}{r} + \tau_{rz}^{nl}\left(\frac{\partial u^*}{\partial z} + \frac{\partial v^*}{\partial r}\right)\right) r\, dr\, dz \tag{34}$$

Subsititute eq. (34) into eq. (33) gives:

$$C_i u_i \mathbf{e}_r + C_i u_i \mathbf{e}_r + \int_{\Gamma}\left(t_r^*\, u + t_z^*\, v\right) r\, d\Gamma = \int_{\Gamma}\left(t_r^l\, u^* + t_z^l\, v^*\right) r\, d\Gamma + \int_{\Gamma} (t_r^{nl}\, u^* + t_z^{nl}\, v^*)\, r\, d\Gamma - \iint_{\Omega}\left(\sigma_r^{nl}\frac{\partial u^*}{\partial r} + \sigma_z^{nl}\frac{\partial v^*}{\partial z} + \sigma_\theta^{nl}\frac{u^*}{r} + \tau_{rz}^{nl}\left(\frac{\partial u^*}{\partial z} + \frac{\partial v^*}{\partial r}\right)\right) r\, dr\, dz \tag{35}$$

Noting that:

$$t_r = t_r^l + t_r^{nl} = \sigma_r n_r + \tau_{rz} n_z$$
$$t_z = t_z^l + t_z^{nl} = \tau_{rz} n_r + \sigma_z n_z$$

Then, eq. (35) gives:

$$C_i u_i \mathbf{e}_r + C_i u_i \mathbf{e}_r + \int_\Gamma \left(t_r^* u + t_z^* v\right) r\, d\Gamma = \int_\Gamma \left(t_r\, u^* + t_z\, v^*\right) r\, d\Gamma + \iint_\Omega \left(\sigma_r^{nl} \frac{\partial u^*}{\partial r} + \sigma_z^{nl} \frac{\partial v^*}{\partial z} + \sigma_\theta^{nl} \frac{u^*}{r} + \tau_{rz}^{nl} \left(\frac{\partial u^*}{\partial z} + \frac{\partial v^*}{\partial r} \right) \right) r\, dr\, dz \quad (36)$$

Similarly, as performed in the small deformation derivations, u^* and v^*, considering each direction independently, may be written as:

$$u^* = U_{rr}\mathbf{e}_r + U_{zr}\mathbf{e}_z, \text{ and } v^* = U_{rz}\mathbf{e}_r + U_{zz}\mathbf{e}_z .$$

similarly, the traction vector components at the field point *Q* can be expressed as;

$$t_r^* = T_{rr}\mathbf{e}_r + T_{zr}\mathbf{e}_z, \text{ and } t_z^* = T_{rz}\mathbf{e}_r + T_{zz}\mathbf{e}_z.$$

Substitute the above equations into eq. (36), and simplified the final boundary integral equation will be given in a matrix form as;

$$\begin{bmatrix} C_{rr} & C_{rz} \\ C_{zr} & C_{zz} \end{bmatrix} \begin{bmatrix} u^i \\ v^i \end{bmatrix} + \int_\Gamma \begin{bmatrix} T_{rr} & T_{rz} \\ T_{zr} & T_{zz} \end{bmatrix} \begin{bmatrix} u \\ v \end{bmatrix} r\, d\Gamma = \int_\Gamma \begin{bmatrix} U_{rr} & U_{rz} \\ U_{zr} & U_{zz} \end{bmatrix} \begin{bmatrix} t_r \\ t_z \end{bmatrix} r\, d\Gamma + \iint_\Omega \begin{bmatrix} \sigma_r^{nl} \frac{\partial U_{rr}}{\partial r} + \sigma_z^{nl} \frac{\partial U_{rz}}{\partial z} + \sigma_\theta^{nl} \frac{U_{rr}}{r} + \tau_{rz}^{nl} \left(\frac{\partial U_{rr}}{\partial z} + \frac{\partial U_{rz}}{\partial r} \right) \\ \sigma_r^{nl} \frac{\partial U_{zr}}{\partial r} + \sigma_z^{nl} \frac{\partial U_{zz}}{\partial z} + \sigma_\theta^{nl} \frac{U_{zr}}{r} + \tau_{rz}^{nl} \left(\frac{\partial U_{zr}}{\partial z} + \frac{\partial U_{zz}}{\partial r} \right) \end{bmatrix} r\, dr\, dz \quad (37)$$

Equation (37) represents the final boundary integral equation for the large strain elastomeric materials. The boundary integral terms can be evaluated numerically by descretising the boundary of the problem. Whereas, the domain integral terms required the domain to be descretised in similar manner as usually used in the finite element techniques.

BOUNDARY ELEMENT FORMULATION

Small Deformation BE Formulation

In small deformation analysis, the problem is considered to be for linear elastic axisymmetric solids. Therefore as stated previously only the boundary of the radial plane has to be discretised. In order to solve the integral equations numerically the boundary, Γ, of the domain, eq. (21) will be discretized into a number of boundary elements over which the displacements and traction are written in terms of nodal points, and the numerical integration performed over each elements and added together.

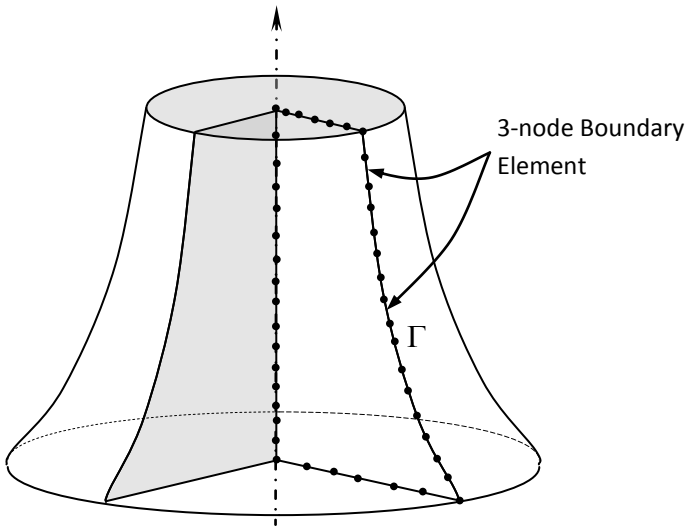

Figure 3: Discretisation of the boundary of linear axisymmetric solid into M_B quadratic element.

After discretising the boundary into M_B elements, eq. (21) may be rewritten, in the absence of body forces, as:

$$\begin{bmatrix} C_{rr} & C_{rz} \\ C_{zr} & C_{zz} \end{bmatrix} \begin{bmatrix} u^i \\ v^i \end{bmatrix} + \sum_{j=1}^{M} \int_{\Gamma_j} \begin{bmatrix} T_{rr} & T_{rz} \\ T_{zr} & T_{zz} \end{bmatrix} \begin{bmatrix} u \\ v \end{bmatrix} r_Q \mathrm{d}\Gamma_j = \sum_{j=1}^{M} \int_{\Gamma_j} \begin{bmatrix} U_{rr} & U_{rz} \\ U_{zr} & U_{zz} \end{bmatrix} \begin{bmatrix} t_r \\ t_z \end{bmatrix} r_Q \mathrm{d}\Gamma_j \tag{38}$$

In a matrix form

$$\mathbf{C}^i \mathbf{u}^i + \sum_{j=1}^{M_B} \int_{\Gamma_j} \mathbf{T}\,\mathbf{u}\; r_Q \mathrm{d}\Gamma_j = \sum_{j=1}^{M_B} \int_{\Gamma_j} \mathbf{U}\;\mathbf{t}\; r_Q \mathrm{d}\Gamma_j \tag{39}$$

or in terms of the shape functions as:

$$\mathbf{C}^i \mathbf{u}^i + \sum_{j=1}^{M_B} \left[\int_{\Gamma_j} \mathbf{T}\, \boldsymbol{\mathcal{F}}\, r_Q \mathrm{d}\Gamma_j \right] u_j = \sum_{j=1}^{M_B} \left[\int_{\Gamma_j} \mathbf{U}\; \boldsymbol{\mathcal{F}}\, r_Q \mathrm{d}\Gamma_j \right] t_j \tag{40}$$

where

$$\mathbf{T} = \begin{bmatrix} T_{rr} & T_{rz} \\ T_{zr} & T_{zz} \end{bmatrix}; \quad \mathbf{U} = \begin{bmatrix} U_{rr} & U_{rz} \\ U_{zr} & U_{zz} \end{bmatrix}$$

And $\boldsymbol{\mathcal{F}}$ is the shape function matrix.

LARGE DEFORMATION BE FORMULATION

In this section elastomeric problem with large deformation is considered. It is noted that eq. (37) contains both boundary integral terms and domain integral terms. The boundary integral terms require the discretisation of the boundary in order to evaluate it. Thus, the boundary of the problem is discretised into boundary elements. The domain terms require the domain to be subdivided into cells or elements to evaluate the integrals. In this work the domain of the problem is discretised using 8-nodes isoparametric elements.

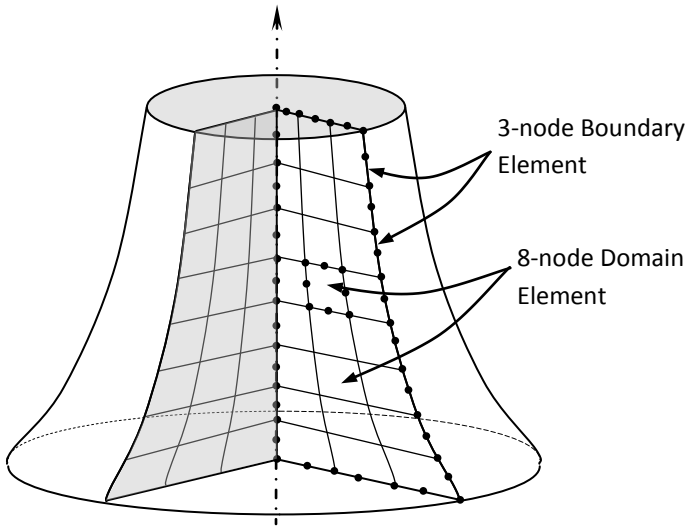

Figure 4: Discretisation of the boundary into M_B quadratic element, and the domain into M_D 8-node element.

To evaluate eq. (37) numerically, it is required that the boundary 'Γ' of the domain, and the domain of the problem to be discretised into boundary elements and domain cells, repectively. The boundary and the domain discretisation are shown in Fig. 4.

After discretising the boundary into M_B elements and the domain into M_D elements, equation (37) can be rewritten in a discretised form as:

$$\mathbf{C}^i\mathbf{u}^i + \sum_{j=1}^{M_B}\int_{\Gamma_j}\mathbf{T}\,\mathbf{u}\; r_Q \mathrm{d}\Gamma_j = \sum_{j=1}^{M_B}\int_{\Gamma_j}\mathbf{U}\;\mathbf{t}\; r_Q \mathrm{d}\Gamma_j + \sum_{j=1}^{M_D}\iint_{\Omega_j}\mathbf{D}\, r\, dr\, dz \tag{41}$$

where

$$\mathbf{D} = \begin{bmatrix} \sigma_r^{nl}\dfrac{\partial U_{rr}}{\partial r} + \sigma_z^{nl}\dfrac{\partial U_{rz}}{\partial z} + \sigma_\theta^{nl}\dfrac{U_{rr}}{r} + \tau_{rz}^{nl}\left(\dfrac{\partial U_{rr}}{\partial z} + \dfrac{\partial U_{rz}}{\partial r}\right) \\ \sigma_r^{nl}\dfrac{\partial U_{zr}}{\partial r} + \sigma_z^{nl}\dfrac{\partial U_{zz}}{\partial z} + \sigma_\theta^{nl}\dfrac{U_{zr}}{r} + \tau_{rz}^{nl}\left(\dfrac{\partial U_{zr}}{\partial z} + \dfrac{\partial U_{zz}}{\partial r}\right) \end{bmatrix}$$

or in terms of the shape function matrices as;

$$\mathbf{C}^i\mathbf{u}^i + \sum_{j=1}^{M_B}\left[\int_{\Gamma_j}\mathbf{T}\,\boldsymbol{\mathcal{F}}\, r_Q \mathrm{d}\Gamma_j\right]\mathbf{u}_j = \sum_{j=1}^{M_B}\left[\int_{\Gamma_j}\mathbf{U}\;\boldsymbol{\mathcal{F}}\, r_Q \mathrm{d}\Gamma_j\right]\mathbf{t}_j + \sum_{j=1}^{M_D}\iint_{\Omega_j}\mathbf{D}\, r\, dr\, dz \tag{42}$$

Solution Algorithm

Eq. (42) may be written as

$$\mathbf{C}^i\mathbf{u}_c^i + \sum_{j=1}^{M_B}\hat{\mathbf{H}}_{ij}\mathbf{u}_j = \sum_{j=1}^{M_B}\mathbf{G}_{ij}\mathbf{t}_j + \sum_{j=1}^{M_D}\mathbf{D}_{ij} \tag{43}$$

Define

$$\mathbf{H}_{ij} = \begin{cases} \hat{\mathbf{H}}_{ij} & if \quad i \neq j \\ \hat{\mathbf{H}}_{ij} + \mathbf{C}^i & if \quad i = j \end{cases}$$

Therefore, eq. (43) will be written as:

$$\sum_{j=1}^{M_B}\mathbf{H}_{ij}\mathbf{u}_j = \sum_{j=1}^{M_B}\mathbf{G}_{ij}\mathbf{t}_j + \sum_{j=1}^{M_D}\mathbf{D}_{ij} \tag{44}$$

And the global system of equations is written as,

$$\mathbf{H}\,\mathbf{u} = \mathbf{G}\,\mathbf{t} + \mathcal{D} \tag{45}$$

Applying the boundary condition and rearranging the columns in **H** and **G** matrix, eq. 45 can be rewritten as:

$$\mathbf{A}\,\mathbf{X} = \mathbf{Y} + \mathcal{D} \tag{46}$$

It can be seen that the boundary integral equations involves a non-linear term, which is a function of the displacement derivatives and the hydrostatic pressure. With the above equations it is possible to formulate the iterative solution procedure for non-linear boundary element analysis as follows. From eq. (45) it can be seen that non-linear terms are involved which are a function of the displacement derivatives and hydrostatic pressure. The dependence of this term on the hydrostatic pressure and the displacement derivatives stems from the term's involvement of the first Piola-Kirchhoff stress (total stress) in its derivative. These non-linear terms can be seen to augment the force/traction vector **Y** in eq. (46), the reduced system of equations after prescribed boundary conditions have been applied. Thus a solution to eq. (46) must involve an iterative solution procedure.

As with most iterative solution procedures the first step is to solve the equivalent linear problem to obtain an initial estimate of the solution. This involves solving eq. (46) but ignoring the domain term with the non-linear stresses i.e. $\mathcal{D} = \mathbf{0}$. The solution vector to this equation can then be used to evaluate the displacement derivatives and hydrostatic pressures to use in the full non-linear boundary integral equations including the non-linear term.

Evidently this first solution vector, and subsequent solution vectors before convergence, will not fully satisfy the full non-linear set of boundary integral equations and a residual or error value will result if the solution vector is substituted back into eq. (46). This residual can be reduced if a new

set of hydrostatic pressures and stresses are calculated based on the previous iteration results. These values can then be used to compute new non-linear domain terms to augment the standard linear BIE force vector. The solution to this set of equations will result in an improved vector of total nodal displacements and tractions. The difference between the new solution vector and the old one gives the iterative improvement in the solution vector. This process is repeated until the ratio of the square of the solution vector increment over the square of the total solution vector results in a value less than a given permissible, as depicted in Fig. 5a.

Incremental Modification to the Solution Algorithm

In the preceding section the basic iterative solution procedure was explained. It is the case that for non-linear problems the only way to achieve convergence of the iterative process for most load cases is to break the applied load down into load increments. This is certainly the only way to achieve convergence for the type of non-linear hyperelastic stress, Bayliss 2004. Therefore it is essential to develop an incremental version of the basic iterative solution algorithm. This can be achieved with the following algorithm shown in Fig. 5b.

As is usual for most non-linear numerical algorithms the first iteration of the first increment is the solution of the equivalent linear problem. The next part of the algorithm is as discussed in the preceding section where by the previous solution vector (tractions and displacements) is used to evaluate the displacement derivatives, and therefore, to enable the non-linear stresses to be found so as to compute the nonlinear domain terms in the system of boundary integral equations.

The significant difference however with the incremental algorithm is that for each iteration the 'old' and 'new' values of the solution vector and the non-linear stresses (at each domain Gauss point and at each source point) are stored. Therefore the total solution vector is formed from the total cumulative sum of the change in displacements and tractions at each iteration of each increment. The change in non-linear stress, or the difference between the current and previous iteration values, is used in the non-linear domain term. This means that for each increment the non-linear domain term reduces for each iteration until convergence occurs. Therefore this algorithm is pseudo incremental because at each iteration of every increment the system of boundary integral equations are still solved for the total displacements and tractions, Bayliss 2004 and Burn *et. al.* 2003.

Because the geometry is always changing as the displacements become large due increments of larger loads, therefore some additional steps are required. Because the boundary integral derivations are based on 1st Piola-Kirchhoff stress values the prescribed tractions (surface stresses) need to be converted to 1st Piola-Kirchhoff values, which will start to differ from nominal values as the strain increases.

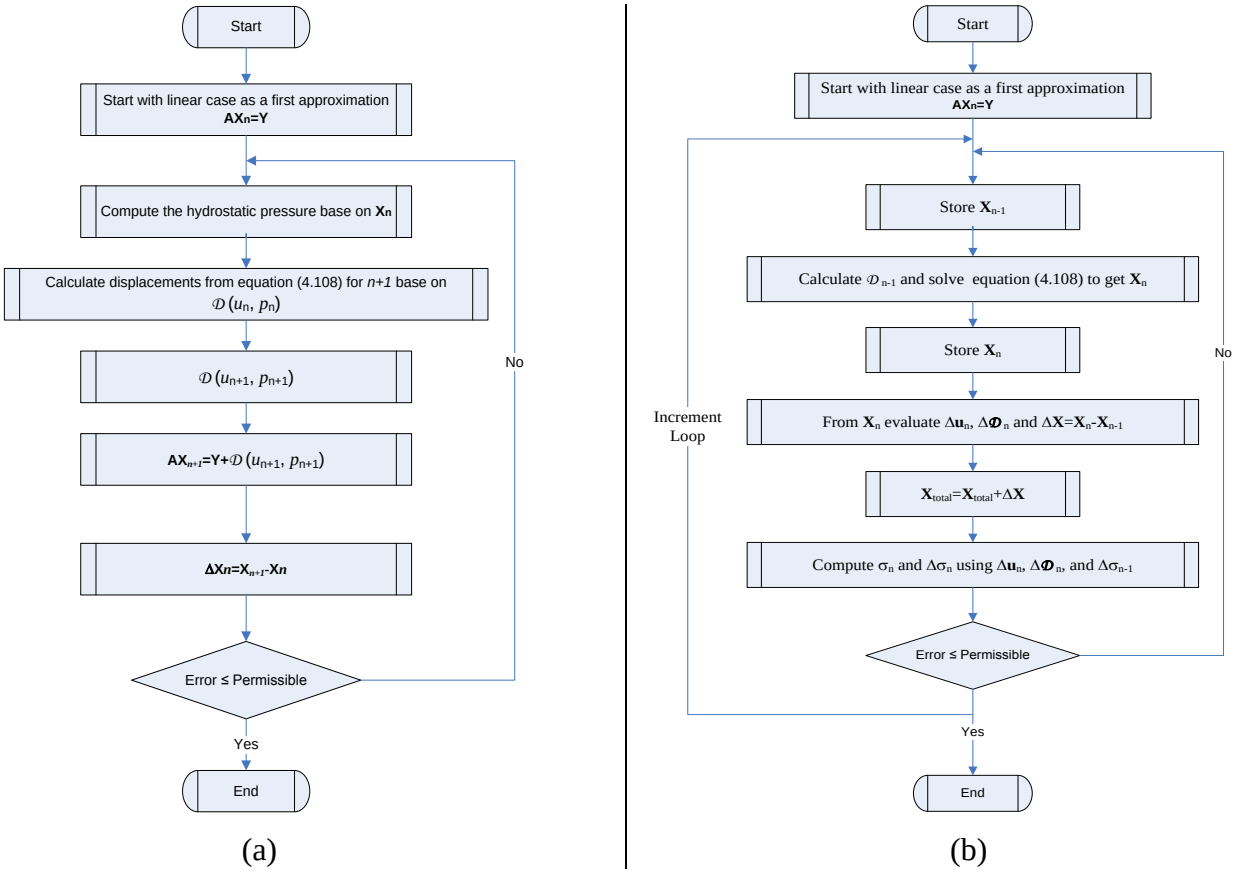

Figure 5: (a) Iterative solution procedure for non-linear boundary integral equations;
(b) Incremental modification to iterative solution procedure.

SMALL DEFORMATION OF INCOMPRESSIBLE MATERIALS

Compression of Bonded Rubber Block

In this example the deformation due to compression of bonded thin rubber block, which is widely used as spring, is studied. The rubber block, as shown in Fig. 6, is bonded on its major surfaces to rigid plates. Gent and Lindley, 1959, assumed that the deformation takes place in two stages: a pure homogeneous compression of amount *e*, requiring a uniform compressive stress $\sigma=3Ge$, *i.e.* $\upsilon=0.5$, and a shear deformation restoring points in the planes of the bonded surfaces to their original positions in these planes.

The material is completely incompressible with a Poisson's ratio of 0.5 exactly. The numerical values are chosen to be: e=10%h, (a/h)=4.5, υ=0.5, and E=23 N/mm^2. The problem is solved by boundary element method of the present work and compared with the finite element software ANSYS Release 10.0. The boundary of the problem is discretised with 22 quadratic 3-node boundary elements with total number of nodes of 45. The Poisson's ratio is chosen of 0.5 exactly. While for the ANSYS the Poisson's ratio has to be approximated as close as 0.5. Firstly, the value is chosen as 0.49 and, secondly as 0.49999 with element type 183 of 8-node, the problem is solved as axisymmetric solid with mixed u/p (displacement/pressure). In ANSYS the Poisson's ratio has to be approximated as 0.49+, exact value of 0.5 is not allowed.

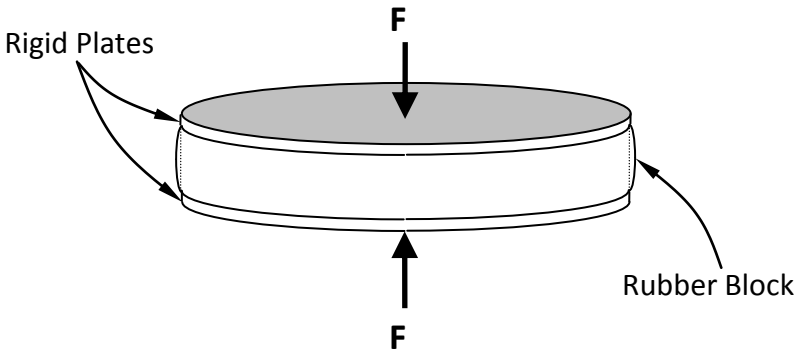

Figure 6: Compression of bonded rubber block

The results from the boundary element methods of the present work are compared with that of the analytical solution of Gent and Lindley 1959, as shown in Fig. 7. On the same graph the finite element results from ANSYS are plotted with Poisson's ratio of 0.49 and 0.49999. From this graph it is shown that the boundary element results are in good agreement with that of analytical solution. While for ANSYS the results are very sensitive to the chosen value of Poisson's ratio. For ANSYS selecting Poisson's ratio value close to 0.5 gives us better results.

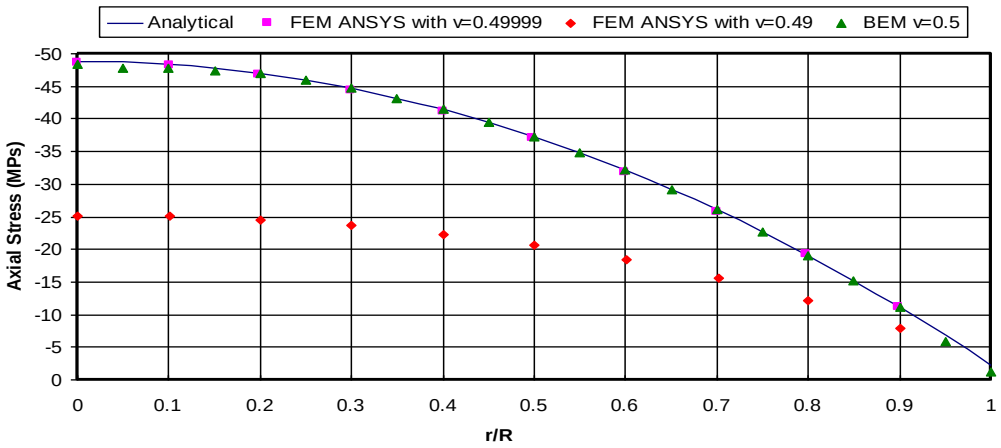

Figure 7: Axial stress for bonded rubber block

AXISYMMETRIC PRESSURE VESSEL

In this example an epoxy flat-headed pressure vessel subjected to internal pressure of 2.61 psi of a dimension shown in Fig. 8, is considered. Floyd, 1984, analyzed this vessel using experimental and theoretical analysis. The experimental Floyd's pressure vessel was made of epoxy resin, which is an almost incompressible material (ν=0.5), the experimental analysis was performed using photo-elastic model and all the stresses are computed along the line BE, as shown in Fig. 8.

The problem is solved numerically using boundary elements method of the present work, and compared with finite element solution using ANSYS 10.0. The boundary elements mesh used is of 38 of 3-node quadratic elements. The boundary conditions are as follows: The material originally on the axis of rotation was constrained to remain on the center line (i.e. u=0) and the material of vessel along CD is constrained to move only in horizontal direction (i.e. v=0). These boundary conditions properly reflect the symmetry of the problem.

The stress results from boundary elements solution of the present work are compared with corresponding values obtained from and ANSYS 10.0, and these results are compared with Floyd's

experimental (photo-elastic) results obtained by at the inner and outer surface of a line of interest (BE), as shown in the following table.

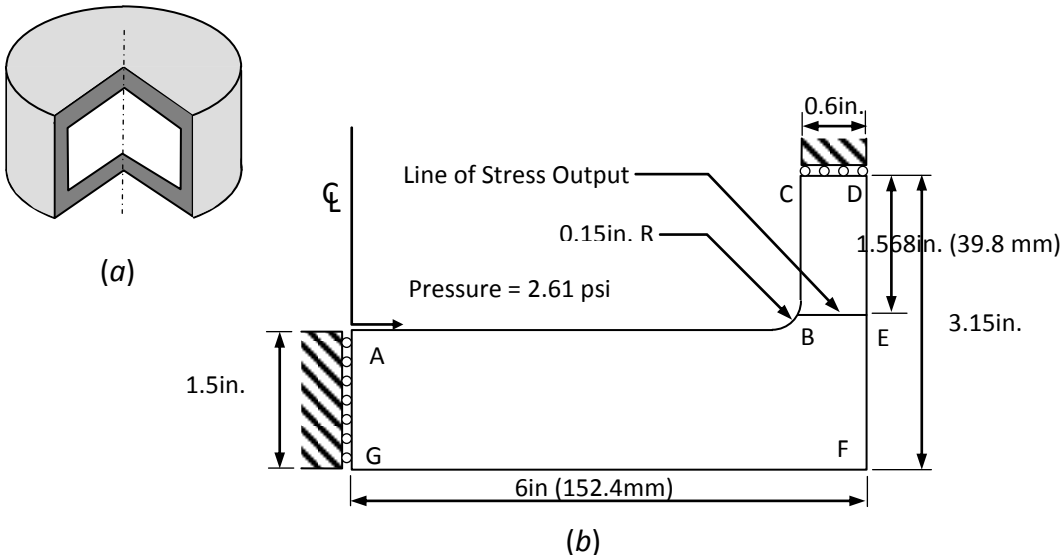

Figure 8: Axisymmetric pressure vessel geometry. (*a*) Schematic drawing. (*b*) Dimensions

Principal Stresses		Floyd 1984 Experimental	BEM Present Work	ANSYS 10.0 υ=0.49	ANSYS 10.0 υ=0.49999
σ_3	Inner surface	2130	2101	2344	2398
	Outer surface	-1000	-990	-1022	-1029
σ_2	Inner surface	-138	-203	299	291
	Outer surface	-1517	-1476	-1356	-1348
σ_1	Inner surface	5310	5320	5308	5291
	Outer surface	0	0	-15	-13

The analysis using ANSYS required refined mesh near the fillet to produce results of sufficient accuracy. While for the boundary elements method it is only requires very simple data input with small number of elements to attain accurate results. It is seen from the above table that the results from the boundary elements method of the present work gives accurate results compared with the experimental analysis. And these results are better than ANSYS results with comparatively very little total number of nodes. The Poisson's ratio used in the boundary element data input is 0.5 exactly, while in the finite element, i.e. ANSYS, it has to be approximated as 0.49+, in the same table the results is given for the finite element with 0.49 as a first case and 0.49999 as a second case. It is seen from these results that the chosen value of the approximated Poisson's ratio affect the results significantly and the results are not converged as increasing the value from 0.49 to as close value as near 0.5, and the question arises if there is a specific value of approximated Poisson's ratio that gives better results?

LARGE DEFORMATION ANALYSIS

Large Deformation of Rubber Cylinder

In this example a rubber thick cylinder of a finite length subjected to internal pressure is studied, the cylinder is considered as an axisymmetric hyperelastic solid and solved via finite and boundary element methods.

Shi Shouxia and Yang Jialing 1999 studied an infinite rubber cylinder subjected to internal pressure, the analyses type used was by considering two dimensional plane strain finite deformation. They solved the problem using Yeoh's hyperelastic constitutive model.

The dimensions and geometry of the rubber cylinder, shown in Fig. 9, are chosen to coincide with that of Shi Shouxia and Yang Jialing 1999. Therefore, the inner radius, R_i, is 70 mm; and R_o=186 mm and, contrarily, the length is chosen to be of finite length, viz. L=500 mm. The cylinder is subjected to internal pressure P.

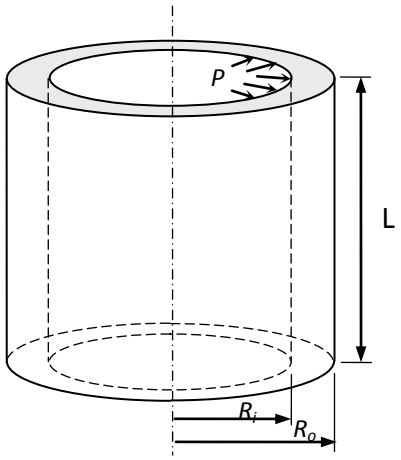

Figure 9: Dimensions and geometry of rubber cylinder

The problem was solved by using both the boundary elements method of the present work, which based on Mooney-Rivlin hyperelastic constitutive model. And using finite element methods via ANSYS 10.0. The material properties are assumed to be of Treloar, 1975, experimental data, and the stretch ratio is limited to 3. The material coefficients are calculated as: c_{10}=1.37890 and c_{01}=0.324855.

The results of the radial displacement is plotted agianst radial distance, as shown in Fig. 10, for both boundary elements and finite element using ANSYS. It is seen from the figure that the boundary element results is in good agreement with that of ANSYS especially when the pressure value is low, and as the value of the pressure increases the difference between the results of the boundary and finite element is slightly increases. And for internal pressure value of 3 MPa, the radial displacement is near 125 mm which gives a stretch ratio of approximately 2 in hoop, therefore the results of the constructed boundary elements program gives satisfactory values for both small and large deformations as compared with ANSYS.

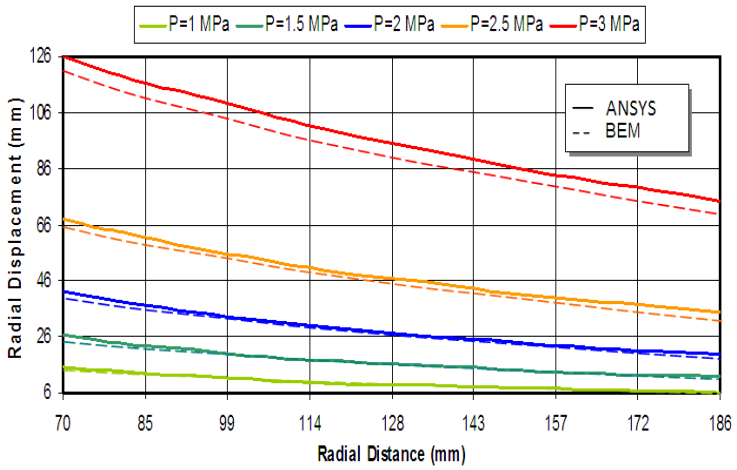

Figure 10: Radial displacement vs radial distance for rubber cylinder subjected to different values of internal pressure.

Figure 11 shows the results of the radial and hoop stresses along the radial distance for different values of internal pressure for both boundary elements and finite element using ANSYS. It is seen from the figure that results are in good agreement for both boundary and finite elements.

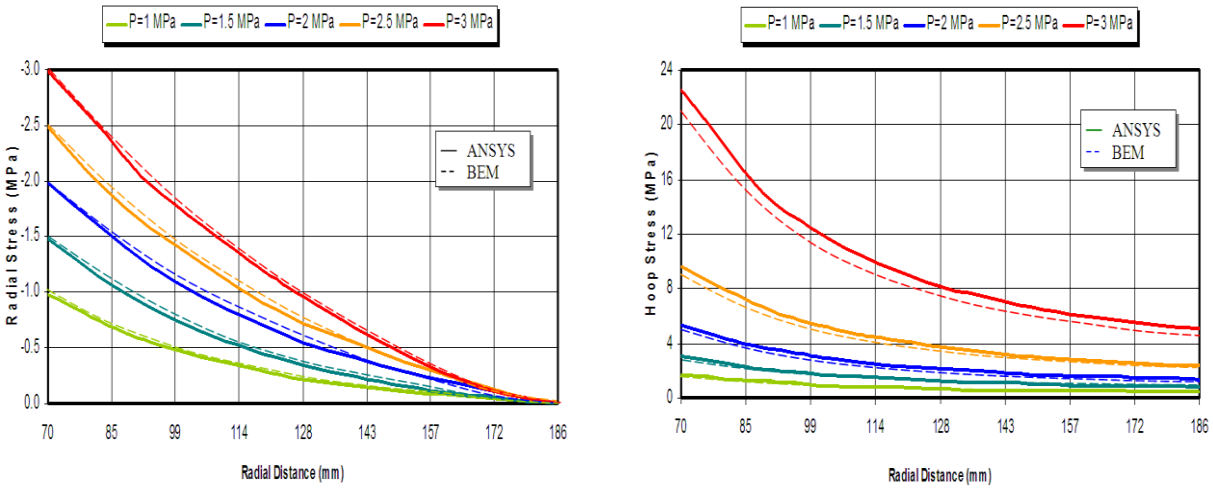

Figure 11: Radial and Hoop stresses versus radial distance for rubber cylinder subjected to different values of internal pressure.

Generally, for both FEM and BEM numerical results, it can be seen that good agreement of the results is obtained and that the expected shape of displacement and stress distribution is correct. Specifically, the radial stress is equal and opposite to the internal pressure on the internal radius and zero radial stress on the outer radius. And the absolute value of hoop stress at all radial position is greater than the absolute values of the radial stresses.

CONCLUSIONS

The following conclusions have been made regarding the use of the boundary elements method for solving elastomeric problems:

- The boundary element method is shown to be good and useful numerical technique for solving problems of incompressible elastomeric materials. The numerical results are improved by handling singularities using some sort of transformation or redistribution techniques for the Gauss integration points.
- In using this method there is no need to approximate the Poisson's ratio as required in the finite element techniques.
- The formulation for the large strain analysis is based on decomposing the 1st Piola-Kirchhoff stress into linear and nonlinear parts. For the non-linear analysis the incremental procedure is used with an iterative algorithm.
- Comparing the results with the available ones or with ANSYS 10.0 shows that this technique is satisfactory approximation and gives good results.

REFERENCES

- Bayliss, M.T., and El-Zafrany A. "Numerical modeling of elastomers using the boundary element method," *Commun. numer. methods eng*. vol. 20, 789-799, 2004.
- Brebbia, C. and Dominguez, J., *Boundary Element: An Introductory Course*, McGraw-Hill, 1989.
- Burn, M., Capuani, D. and Bigoni, D., "A boundary element technique for incremental, non-linear elasticity," Part I: Formulation, *Comput. Methods Appl. Mech. Engrg.* 192, 2461-2479, 2003.
- Floyd, C.G., "The determination of stress using combined theoretical and experimental measurements," *Proc. 2nd int. Conf.*, Ed. C.A. Brebbia, 1984.
- Fung, Y.C., *Foundations of Solid Mechanics*, Prentice-Hall, Inc., Englewood Cliffs, NJ, 1965.
- Herrmann, L.R., "Elasticity Equations for Incompressible and nearly Incompressible Materials," *AIAA J. 3(10),* 1896-1900, 1985.
- Gent, A.N., *Engineering with Rubber: How to Design Rubber Components*, Hanser Publishers, 2001.
- Gent, A.N., and Lindley, P.B., "The compression of bonded rubber blocks," *Proc. I. Mech. E.*, 173: 111-117, 1959.
- Kyuichiro Washizo, *Varitional Method in Elasticity and Plasticity*, Pergamon Press,1975.
- Polyzos, D., Tsinopoulos, S. V., and Beskos, D. E., "Static and Dynamic Boundary Element Analysis in Incompressible Linear Elasticity", *Eur. J. Mech. Solids 17*, 515-536, 1998.
- Rizzo, F. J. and D. J. Shippy, "A Boundary Element Method for Axisymmetric Elastic Bodies*",* in *Developments in Boundary Element Mothods-4*, Eds. P.K. Banerjee, & J.O Watson, 1986.
- Shi Shouxia and Yang Jialing, "Large deformation of incompressible rubber cylinder under plane strain," *ACTA Mechanica Solida Sinica*, Vol. 12, No. 4, December 1999.

- Treloar, L. R. G., *The Physics of Rubber Elasticity*, 3rd Edition, Clarendon Press, Oxford, 1975.

NOMENCLATURE

C_{ij}	Cauchy principal value	
E	Modulus of elasticity	N/m^2
$\boldsymbol{F}$	Shape function matrix	
G	Shear modulus	N/m^2
n_r , n_z	Direction cosines of the outward normal $\hat{n}$	
t	Traction components	N/m^2
T_{ij}	Traction kernel functions	
u	Displacements components	m
U_{ij}	Displacement kernel functions	
ε_r , ε_θ , ε_z	Strains in r, θ, z direction	
σ_r , σ_θ , σ_z	Stresses in r, θ, z direction	N/m^2
β_r	Radial components of the body force	
β_z	Axial components of the body force	
δ_{ij}	Krönecker delta	
ϕ_i	Interpolation (shape) function	
Γ	Boundary of the problem	
υ	Poisson's ratio	